Original Research *Highlight article*

Extracellular matrix remodeling is associated with the survival of cardiomyocytes in the subendocardial region of the ischemic myocardium

Qing Chu[1,*], Ying Xiao[1,*], Xin Song[1] and Y James Kang[1,2]

[1]Regenerative Medicine Research Center, Sichuan University West China Hospital, Chengdu, Sichuan 610041, China; [2]Tennessee Institute of Regenerative Medicine, University of Tennessee Health Science Center, Memphis, TN 38163, USA
Corresponding author: Y James Kang. Email: ykang7@uthsc.edu
*These authors contributed equally to this paper.

Impact statement

The subendocardium is highly vulnerable to ischemic insult, yet a significant amount of cardiomyocytes in this region survive under ischemic conditions. This study demonstrates that the extracellular matrix remodeling, including excessive collagen deposition, connexin 43 depletion, and lysyl oxidase elevation, makes these cardiomyocytes electrically isolated, deformed, and resistant to apoptosis under ischemic conditions. These surviving cardiomyocytes could contribute significantly to myocardial repair from ischemic injury, although this remains to be investigated in future studies.

Abstract

A significant amount of cardiomyocytes in subendocardial region survive from ischemic insults. In order to understand the mechanism by which these cardiomyocytes survive, the present study was undertaken to examine changes in these surviving cardiomyocytes and their extracellular matrix. Male C57BL/6 mice aged 8–12 weeks old were subjected to a permanent left anterior descending coronary artery ligation to induce ischemic injury. The hearts were collected at 1, 4, 7, or 28 days after the surgery and examined by histology. At day 1 after left anterior descending ligation, there was a significant loss of cardiomyocytes through apoptosis, but a proportion of cardiomyocytes were surviving in the subendocardial region. The surviving cardiomyocytes were gradually changed from rod-shaped to round-shaped, and appeared disconnected. Connexin 43, an important gap junction protein, was significantly decreased, and collagen I and III deposition was significantly increased in the extracellular matrix. Furthermore, lysyl oxidase, a copper-dependent amine oxidase catalyzing the cross-linking of collagens, was significantly increased in the extracellular matrix, paralleled with the surviving cardiomyocytes. Inhibition of lysyl oxidase activity reduced the number of surviving cardiomyocytes. Thus, the extracellular matrix remodeling is correlated with the deformation of cardiomyocytes, and the electrical disconnection between the surviving cardiomyocytes due to connexin 43 depletion and the increase in lysyl oxidase would help these deformed cardiomyocytes survive under ischemic conditions.

Keywords: Cardiomyocyte survival, extracellular matrix, extracellular matrix remodeling, collagen deposition, lysyl oxidase, subendocardium

Experimental Biology and Medicine **2021; 246: 2579–2588. DOI: 10.1177/15353702211042020**

Introduction

Coronary artery occlusion leads to myocardial infarction, characterized by a significant loss of cardiomyocytes and scar tissue formation, impairing cardiac systolic and diastolic function.[1] It has been found that some cardiomyocytes within the scar tissue remain surviving in animal models, including rats,[2] mice,[3] and dogs,[4] as well as in humans.[4,5] However, changes in morphology and function of the surviving cardiomyocytes remain elusive.

Cardiomyocytes are well-organized and electrically connected, forming the basis for myocardial contraction.[6,7] Extracellular matrix (ECM) in the myocardium is the fundamental support for the physiological connection between cardiomyocytes.[8] Several key elements play critical roles in

the regulation of myocardial ECM. Gap junction alpha-1 protein, or connexin 43 (Cx43), is a major component of the gap junctions that effects electrical connectivity between cardiomyocytes.[9,10] Lysyl oxidase (LOX) is another key regulator of ECM homeostasis and is vital for the structure and function of cardiomyocytes.[8,11,12] LOX is overproduced after myocardial ischemia, followed by an enhanced cross-linking of type I and III collagens in ECM of the affected heart.[12,13] As LOX activation sustains with an excessive collagen deposition, myocardial fibrosis develops leading to cardiac dysfunction.[8,12,14]

Therefore, the changes in ECM in response to myocardial ischemia would have a marked impact on the morphology and function of cardiomyocytes in the same region subjected to ischemic insult. This impact is particularly important for the surviving cardiomyocytes in the highly ischemia-vulnerable subendocardium. In the present study, we assessed possible abnormal changes in the morphology of the surviving cardiomyocytes and their surrounding ECM, paying particular attention to the changes of Cx43 and LOX in response to myocardial ischemia. We found that an enhanced collagen deposition along with an increase in LOX was associated with the survival of cardiomyocytes. In addition, Cx43 was significantly decreased in the remodeling ECM. These together would constitute an electrical isolation of the affected cardiomyocytes, leading to their deformation and resistance to apoptosis under ischemic conditions.

Materials and methods

Animals and animal care

Male C57BL/6 mice of 8 to 12 weeks old, weighing 18–25 g, were obtained from Ensiweier Experimental Animal Breeding and Research Center (Chongqing, China). Mice were fed standard chow (5C02, LabDiet, USA) and tap water *ad libitum*. All animal procedures were approved by the institution animal care and use committee at the Sichuan University, West China Hospital, following the guidelines of the US National Institutes of Health.

Mouse model of myocardial ischemia

Mice were randomly divided into sham-operated ($n = 48$) and myocardial ischemia (MI) groups ($n = 80$). The MI group was subjected to left anterior descending (LAD) artery ligation as described previously.[15] Briefly, mice underwent open chest surgery after anesthesia by isoflurane inhalation. LAD was exposed and a 7-0 suture was pierced beneath, then the LAD was ligated to induce myocardial ischemia. Mice revived shortly after sternal closure. The sham group underwent the same procedure as the MI group, except for LAD ligation. Of the 80 mice undergoing LAD occlusion, 70 survived until the time of sacrifice, and these were used for further investigations.

For the LOX inhibition study, mice were treated with β-aminopropionitrile (βAPN, 100 mg/kg body weight/day; Sigma-Aldrich, A3134), injected intraperitoneally. Control mice received phosphate-buffered saline (PBS) as vehicle control for βAPN.

Tissue preparation

Mice were anesthetized with isoflurane and euthanized in a CO_2 rich cage. Heart samples were collected for histological and molecular analyses. Briefly, the chests were opened and the hearts were removed immediately. After a brief wash in precooled saline (4°C), the atria were removed. Ventricles were split carefully to separate the infarct area for mRNA and protein extraction. For histological analyses, ventricles were split for cross and longitudinal cutting. The tissues were embedded in the optimal cutting temperature compound gel (Leica, German) and frozen in liquid nitrogen for serial frozen sections. The tissues were sectioned at 4 μm intervals and stored at −20°C for immunofluorescent staining. The remaining tissues were fixed in 4% paraformaldehyde and dehydrated in gradient alcohol, embedded in paraffin, then cut into 2.5 μm serial slides for hematoxylin and eosin (HE) staining to observe morphological changes of cardiomyocytes.

For serial sectioning, the whole mount of heart was fixed in 4% paraformaldehyde and then paraffin-embedded. The heart was cut into five 500 μm-thick layers, from the apex to 1 mm above the ligation site, and 2.5 μm sections were collected from each layer for subsequent HE staining to show the surviving cardiomyocytes.

Detection of apoptosis

Apoptotic cell death was detected *in situ* using a terminal deoxynucleotidyl transferase-mediated dUTP-biotin nick end labeling (TUNEL) staining 50 kit (Roche, IN, USA) following the manufacturer's instructions. The tissue sections were fixed with 4% paraformaldehyde for 15 min, washed with PBS for two times, 3 min each time, and treated with a precooled permeabilization solution (0.1% Triton X-100) for 2 min. After washing (PBS for two times, 3 min each time), the labeling reaction was carried out in a solution containing terminal deoxynucleotidyl transferase and fluorescein-dUTP at 37°C for 1 h. Nuclei were counterstained with 4′,6-diamidino-2-phenylindole dihydrochloride (DAPI, Sigma, D9542). TUNEL staining was examined by confocal microscope (ECLIPSE Ti A1, Nikon) with 20× objective lens.

Immunofluorescent staining

Tissue sections were fixed in precooled 4% paraformaldehyde for 15 min and then washed with PBS for three times, 3 min each time. The sections were blocked with 2% bovine serum albumin (BSA) for 1 h at 37°C. Primary antibodies were incubated at 37°C for 1 h followed by incubation at 4°C overnight. Secondary antibodies were incubated at 37°C for 1 h at the concentration of 1/1000. Wheat germ agglutinin (WGA) (lectin from *Triticum vulgaris* wheat, Sigma, L4895, 1:250) staining was incubated as described above, except for the secondary antibody incubation. Nuclei were counterstained with DAPI (Sigma, D9542). Blank control was incubated with 2% BSA instead of primary antibodies. All sections were examined by confocal microscope (ECLIPSE Ti A1, Nikon). At least three fields for each section were captured for each animal unless specifically mentioned.

For three-dimenaional (3D) images of heart, thick tissue (50 μm) was used for immunofluorescent staining, and the primary and second antibodies incubated for 48 h at 4°C. Confocal microscope (ECLIPSE Ti A1, Nikon) was used for 3D reconstruction.

Primary antibodies used were as follows: rabbit anti-mouse Cx43 (1:1000, Abcam, ab11370), rabbit anti-mouse LOX (1:200, Abcam, ab174316), rabbit anti-mouse LOX-PP (1:100, Novus, NB110-41568), goat anti-mouse LOX (1:50, Abcam, ab223488), goat anti-mouse TNNI3 (1:200, Abcam, ab56357), mouse anti-mouse α-actinin (1:200, Abcam, ab9465), rabbit anti-mouse MYH6 (1:200, ABclonal, A9516), rabbit anti-mouse collagen I (1:200, Abcam, ab34710), rabbit anti-mouse collagen III (1:200, Abcam, ab7778), rabbit anti-mouse Ki67 (1:200, Abcam, ab16667), rabbit anti-mouse Nkx2.5 (1:50, Invitrogen, PA5-49431), rabbit anti-mouse myocyte-specific enhancer factor 2C (MEF2C) (1:500, Abcam, ab64644). Secondary antibodies used were as follows: Alexa Fluor 488 goat anti-mouse (Thermo Fisher, A 11001), Alexa Fluor 568 goat anti-mouse (Thermo Fisher, A 11004), Alexa Fluor 488 donkey anti-goat antibody (Thermo Fisher, A 11055), Alexa Fluor 568 donkey anti-goat antibody (Thermo Fisher, A 11057), Alexa Fluor 488 goat anti-rabbit (Thermo Fisher, A 11008), Alexa Fluor 568 goat anti-rabbit (Thermo Fisher, A 11011), Alexa Fluor 647 chicken anti-rabbit (Thermo Fisher, A 21143).

Quantitative reverse transcription polymerase chain reaction (qRT-PCR)

Total RNA was extracted from the myocardium, and then dissolved in Trizol reagent (Invitrogen, USA) according to the manufacturer's instructions. The integrity of total RNA was detected by sepharose gio-gel, and the concentration was quantified using a NanoDrop 2000 spectrophotometer (Thermo Fisher, USA). RNA was reversely transcribed to complementary DNA (cDNA) by using a Prime Scripts RT reagent kit (TaKaRa, Japan) in the MJMini personal thermal Cycler (Bio-Rad, USA). The amount of cDNA corresponding to 50 ng of RNA was amplified using a SYBR green PCR kit (Bio-Rad Laboratories) with the primers. The primer sequences used are listed as follow: *Lox* (forward: ACTTCCAGTACGGTCTCCC, reverse: AGTCTC TGACATCCGCCCTA); *Tbp* (forward: CCTTGTACCCTTC ACCAATGAC, reverse: ACAGCCAAGATTCACGG TAGA).

Statistical analysis

Image J was applied to the analysis of the staining pictures. All data were presented as mean ± SD. GraphPad Prism 7.0 was applied to perform statistical analysis. Two-way ANOVA was used for evaluation of different times post LAD ligation and sham-operation, and Student's *t*-test was followed to compare the difference between the MI group and the sham-operated group. $P < 0.05$ was considered as statistically significant.

Results

Survival of cardiomyocytes in subendocardial region of ischemic myocardium

There was a significant loss of cardiomyocytes measured at day 1 and a further loss at day 4 after LAD ligation, but there was no further loss of cardiomyocytes measured at day 7 after LAD ligation (Figure 1, Figure S1). A proportion of cardiomyocytes in the subendocardial region remained consistently surviving from day 1 to day 28 after LAD ligation (Figure 1(a) to (c), (e)). There was a significantly large number of apoptotic cardiomyocytes detected in the ischemic area at day 1 after LAD ligation, but not so many at days 4 and 7 post ischemic insult. However, in the subendocardial region, there were few apoptotic cardiomyocytes even at day 1 after LAD ligation (Figure 1(d) and (f)).

There were no proliferative cardiomyocytes in the subendocardial region from day 1 to day 7 (Figure 2(a)). However, there were many $Nkx2.5^+$ positive cells which were interfaced with cardiomyocytes at day 1 but which had disappeared by day 7 post ischemic insult (Figure 2 (b)). $MEF2C^+$ cardiomyocytes were detected at day 4 and day 7 (Figure 2(c)), suggesting morphological changes of these surviving cardiomyocytes.

Deformation of the surviving cardiomyocytes in ischemic myocardium

The surviving cardiomyocytes in the subendocardial region were examined from both cross and longitudinal sections (Figure 3(a) and (b)). Normal cardiomyocytes displayed a typical rod-shaped morphology, as demonstrated by round-shaped cross-sections and strip-shaped longitudinal sections, in sham-operated myocardium (Figure 3(b)). The surviving cardiomyocytes in the ischemic myocardium gradually changed their shape from the rod- to round-shaped, as evidenced by there being a gradual change from strip-shaped to round-shaped in longitudinal sections from day 1 to day 7 after LAD ligation (Figure 3(b)). By the seventh day, most of the surviving cardiomyocytes were round-shaped in both cross and longitudinal sections (Figure 3(b)). The sarcomere structure was disturbed, as defined by α-actinin staining (Figure 3(c)). The morphological change was further shown by thick tissue staining followed by 3D reconstruction (Figure 3(d)). When WGA was used to label the membrane of the surviving cardiomyocytes, it was revealed that the total number of cardiomyocytes was significantly decreased in the subendocardial region of the ischemic myocardium relative to that in the sham control (Figure 3(e) and (f)). However, the size of these surviving cardiomyocytes was significantly increased as indicated by the comparable cross-sectional area (CSA) of these surviving cardiomyocytes to that of the sham control (Figure 3(e) and (g)).

ECM remodeling in the subendocardial region of ischemic myocardium

Cx43, a gap junction protein located in the intercalated disc responsible for electrical connection and signal conduction

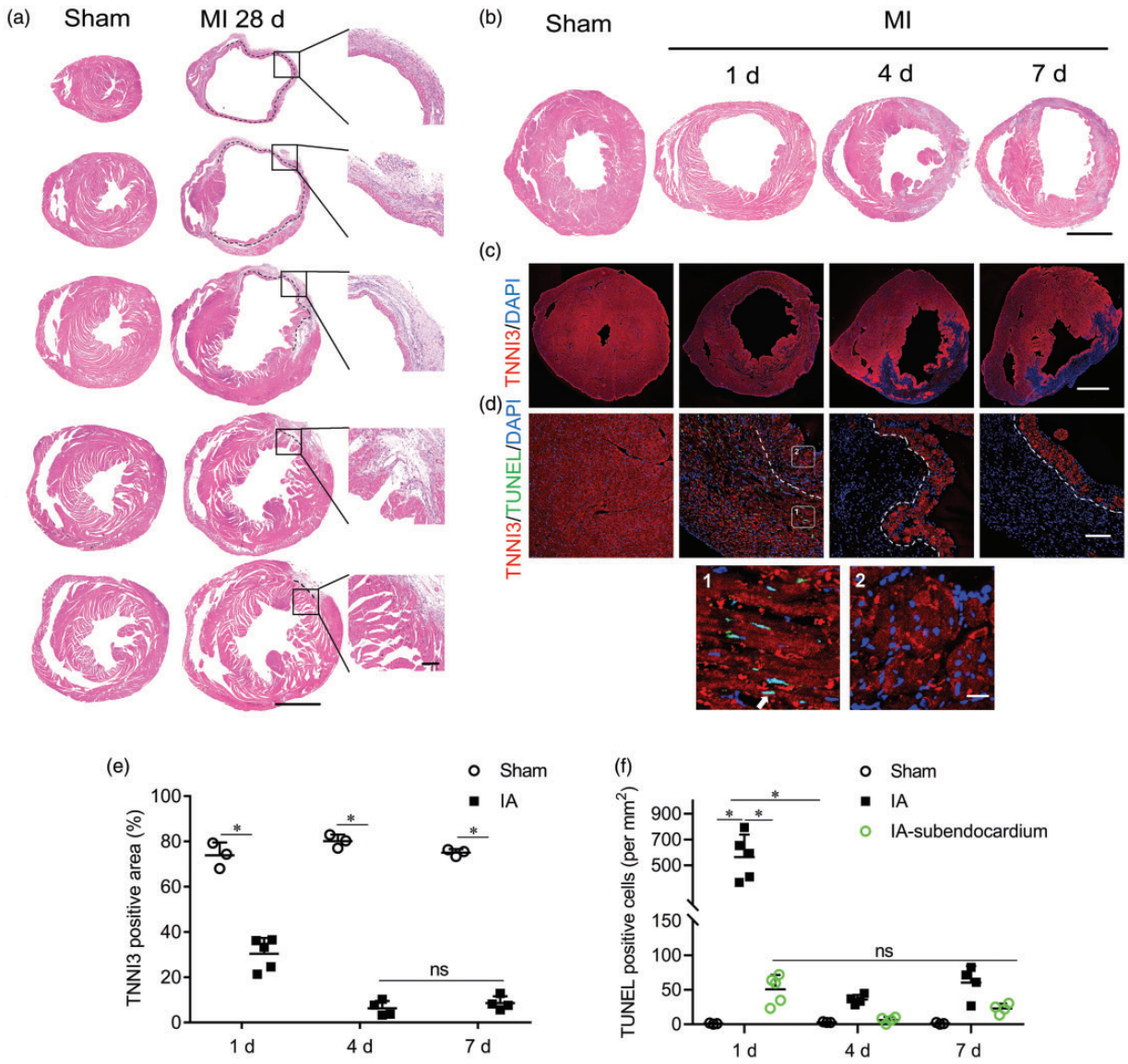

Figure 1. Survival of cardiomyocytes in ischemic myocardium. (a) Serial sectioning of whole heart showing the surviving cardiomyocytes at 28 days after LAD ligation, detected by HE staining. The surviving cardiomyocytes in the sub-endocardial region of the ischemic area (IA) are indicated by dotted lines. Scale bar, 1000 μm and 100 μm. Overview of surviving cardiomyocytes from day 1 to day 7 after LAD ligation, shown by HE staining (b), and immunofluorescent staining (c). Cardiomyocytes are indicated by TNNI3 (red) and nuclei are indicated by DAPI (blue). Scale bar, 1000 μm. Sham: sham-operated control; MI: myocardial ischemia. (d) Apoptosis of cardiomyocytes detected by TUNEL (green) and TNNI3 (red) co-staining in ischemic myocardium. The sub-endocardial region in IA (IA-subendocardium) is indicated by dotted line. Arrow in box 1 indicates apoptotic cells; box 2 represents the apoptotic state in the subendocardial region. Scale bar, 100 μm and 20 μm.
(e) Quantification of TNNI3 positive area (%) in ischemic area (IA). (f) Statistical analysis of TUNEL positive cells in total IA and IA-subendocardium. IA: ischemic area; IA-subendocardium: the sub-endocardial region in IA. *$P < 0.05$ between indicated groups. (A color version of this figure is available in the online journal.)

between cardiomyocytes, was significantly decreased (Figure 4(a) and (b), Figure S2). Collagen I and III were significantly increased and condensed around the surviving cardiomyocytes as measured on day 7 after myocardial ischemia (Figure 4(c) to (f)). The ratio of collagen I/III was decreased at day 1, while returning to the sham-level on day 7 (Figure 4(g)).

Changes in LOX in the subendocardial region of ischemic myocardium

LOX catalyzes the reaction of collagens cross-linking, making ECM maturation. Two isoforms of LOX, LOX-PP and a-LOX (Figure 5, Figure S3) were detected. The protein level of both LOX-PP and a-LOX in the subendocardial region was decreased on day 1 after LAD ligation (Figure 5(a) to (d)). Thereafter, there was a significant increase in both proteins measured either four or seven-days after LAD ligation; there was about a 20-fold increase in LOX-PP (Figure 5(a) and (b)) and a 5-fold increase in a-LOX (Figure 5(c) and (d)). In addition, a redistribution of a-LOX was observed, as it was found in the cytosol and nuclei of the surviving cardiomyocytes (Figure 5(e) to (g), Figure S4). Quantitatively, the proportion of cardiomyocytes containing a-LOX (a-LOX$^+$) was increased from about 15% on day 4 to 40% on day 7 after LAD ligation (Figure 5(f)). To determine if up-regulation of LOX expression was responsible for the increase in LOX proteins, we

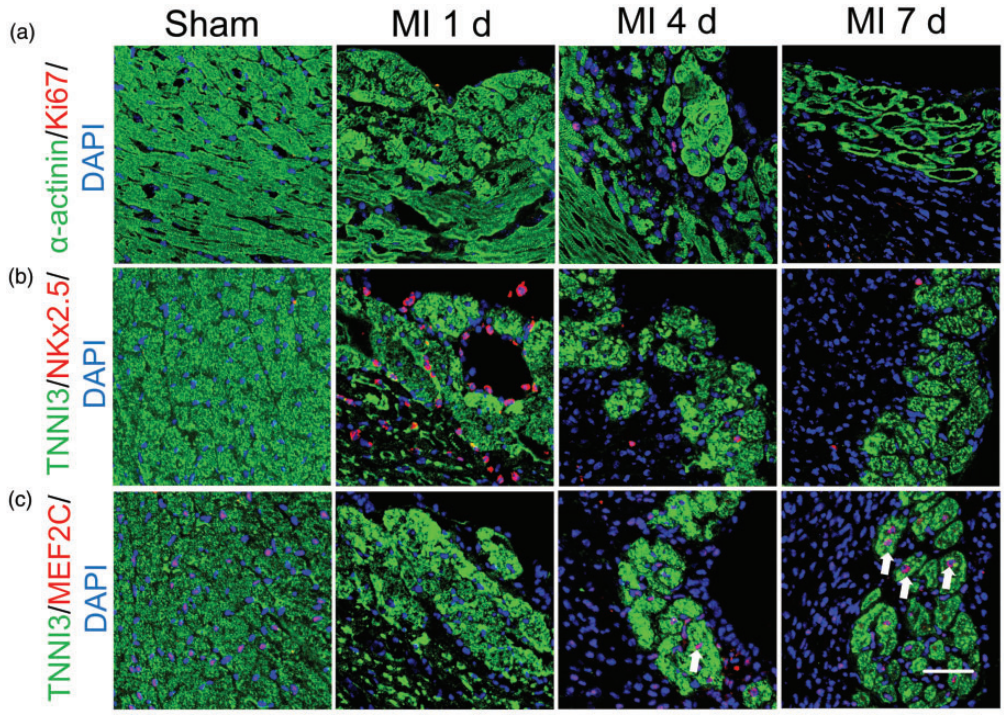

Figure 2. Immunofluorescent staining of the surviving cardiomyocytes. (a) Immunofluorescent staining of Ki67 (red) and α-actinin (green). Nuclei are indicated by DAPI (blue). (b) Immunofluorescent staining of Nkx2.5 (red) and TNNI3 (green). (c) Immunofluorescent staining of MEF2C (red) and TNNI3 (green). White arrow indicates MEF2C^{+} cardiomyocytes at day 4 and day 7 post LAD ligation. Scale bar, 50 μm. (A color version of this figure is available in the online journal.)

measured mRNA levels of LOX. As shown in Figure 5(h), the mRNA level for LOX was significantly increased after four days and further increased after seven days following LAD ligation. To determine the role of the LOX increase in cardiomyocyte survival, we used βAPN (LOX inhibitor) to inhibit LOX activity. As shown in Figure 6(a), βAPN was administered once a day, beginning at day 1 and lasting until day 7 after LAD ligation. This treatment significantly reduced the number of surviving cardiomyocytes in the subendocardium (Figure 6(b) and (c)).

Discussion

Coronary artery occlusion leads to a significant loss of cardiomyocytes in the ischemic myocardium. It has been demonstrated that the subendocardium is at a higher risk of ischemic injury than the midwall or epicardium.[16] However, there are some cardiomyocytes that escape the lethal insult in the subendocardial region.[2–4] Previous study has shown that new vessels developed from the endocardium of the left ventricle salvaged cardiomyocytes in the area.[3] We found here that these surviving cardiomyocytes changed their shape from rod-shaped to round-shaped with their intercellular junction becoming disrupted. These surviving cardiomyocytes were surrounded by an altered ECM with Cx43 depletion and excessive deposition of collagen I and III. LOX, the enzyme catalyzing cross-linking of collagens, was also significantly increased in the remodeled ECM. This remodeling of the ECM would help cardiomyocyte survival but make them deformed in the subendocardial region.

Surprisingly, there were few apoptotic cardiomyocytes in the subendocardial region even at day 1 after LAD ligation, while a large number of cardiomyocytes had undergone apoptosis in other regions of the ischemic myocardium. The subendocardial region is considered more vulnerable to myocardial ischemia than the midwall or epicardium.[17] The remodeling of ECM would help the survival of these cardiomyocytes. On day 1 after LAD ligation, when a large number of apoptotic cardiomyocytes were observed in the ischemic myocardium, Cx43 was decreased in the subendocardial region. Cx43 is a critical component of the intercalated disc that effects electrical continuity between cardiomyocytes, making the myocardium a functional syncytium, and is essential to maintain cardiomyocyte integrity and function.[10,18,19] Previous studies have shown that a mutation or defect in intercalated disc components results in distortions in the structure of cardiomyocytes and leads to cardiac abnormalities.[10,20,21] The reduction of Cx43 would result in electrical disconnection between cardiomyocytes, thus leaving these cells to be electrically isolated, preventing them from responding to communication signals. It was previously reported that a Cx43 inhibitor (Gap26) attenuated LPS-induced apoptosis in H9C2 cells.[22] Thus, these findings taken together suggest that the decreased electrical connectivity due to Cx43 depletion would help protect these cells from apoptosis, although it causes diminished contractility of the heart as a whole.[7,8,23] The rod-shaped of cardiomyocytes is the key characteristic, which is responsible for cardiac contraction.[6] The change of the surviving cardiomyocytes from rod-shaped to round-shaped indicates the reduction in their contractility. Sarcomere structure in these surviving,

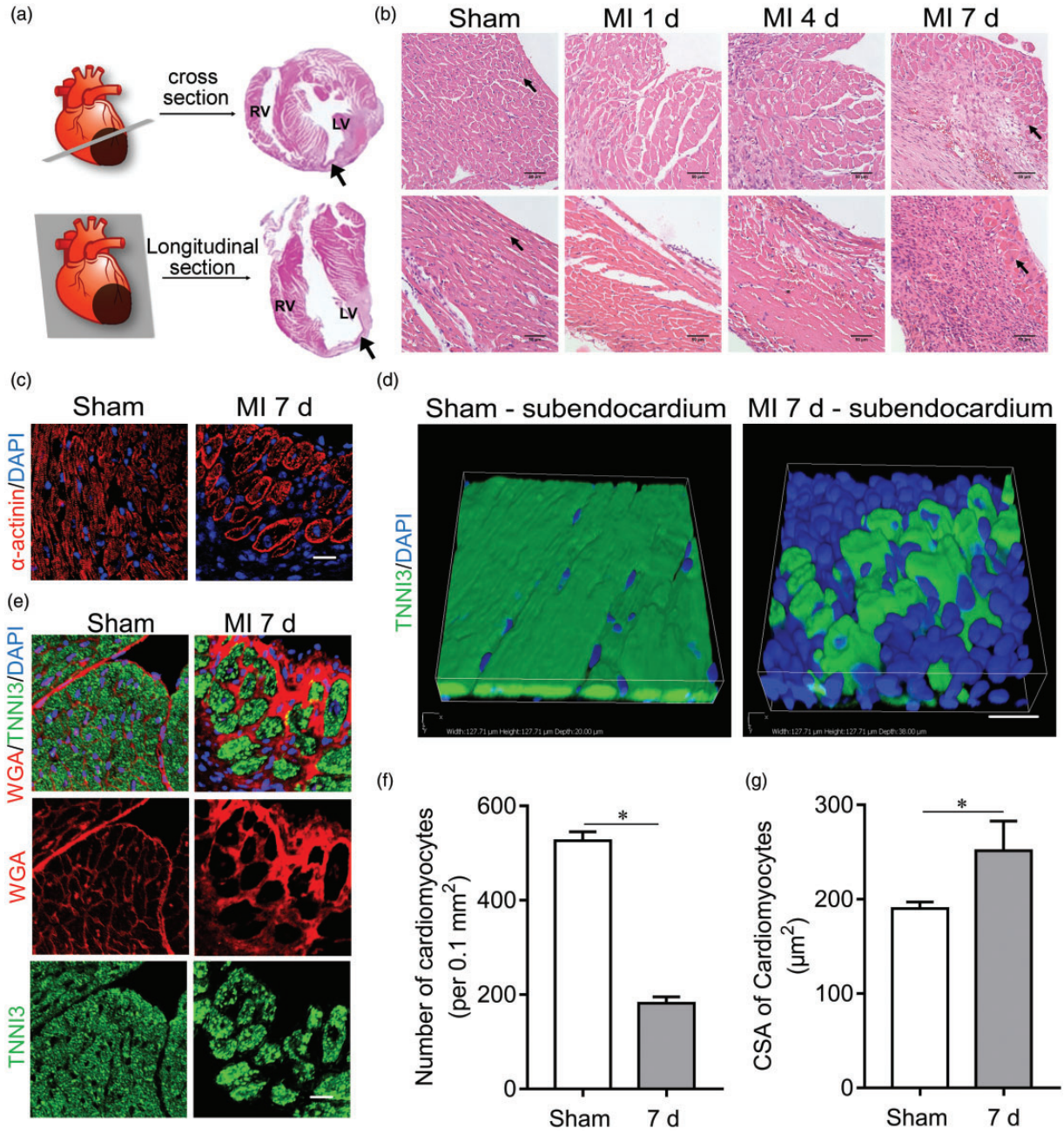

Figure 3. Morphological changes of the surviving cardiomyocytes in ischemic myocardium. (a) Schematic diagram of cross and longitudinal sections preparation. (b) Dynamic morphological alterations of cardiomyocytes from cross and longitudinal sections of hearts from day 1 to day 7 detected by HE staining. Black arrow indicates morphology of normal cardiomyocytes or survived cardiomyocytes, respectively. Scale bar, 50 μm. (c) Immunofluorescent staining of α-actinin (red) shows the sarcomere structure of surviving cardiomyocytes at day 7 after LAD ligation. Nuclei are indicated by DAPI (blue). Scale bar, 20 μm. (d) 3D images of cardiomyocytes in sub-endocardial region in sham-operated control and MI 7 d group. Cardiomyocytes are indicated by TNNI3 (green) and nuclei are indicated by DAPI (blue). Scale bar, 20 μm. (e) Co-immunofluorescent staining of WGA (red) and TNNI3 (green). Nuclei are indicated by DAPI (blue). Scale bar, 10 μm. The number (f) and CSA (g) of cardiomyocytes as depicted and calculated by WGA staining. WGA: wheat germ agglutinin, for labeling the cell membrane; CSA: cross-sectional area. *$P < 0.05$ between indicated groups. (A color version of this figure is available in the online journal.)

rounded cardiomyocytes was disturbed, further indicating the diminished contractile function. Some of these surviving cardiomyocytes also expressed MEF2C, which controls cardiac morphogenesis and myogenesis.[24] It has been previously demonstrated that adult mammalian cardiomyocytes would undergo dedifferentiation, proliferation, and redifferentiation after ischemic injury *in vitro*.[25] The expression of MEF2C in these surviving cardiomyocytes would suggest that the change of cardiomyocytes from being rod-shaped to round-shaped might be reversible with suitable changes in the microenvironment.[7,24]

ECM is the key component in the microenvironment, and ECM alteration disrupts the supporting structure for cell-to-cell communication.[7,14,23,26] We found here that the ECM disruption involved excessive collagen deposition in the ECM, furthering the disconnection between cardiomyocytes. In our previous studies, we observed the activation of fibroblasts in response to the same ischemic insult in the

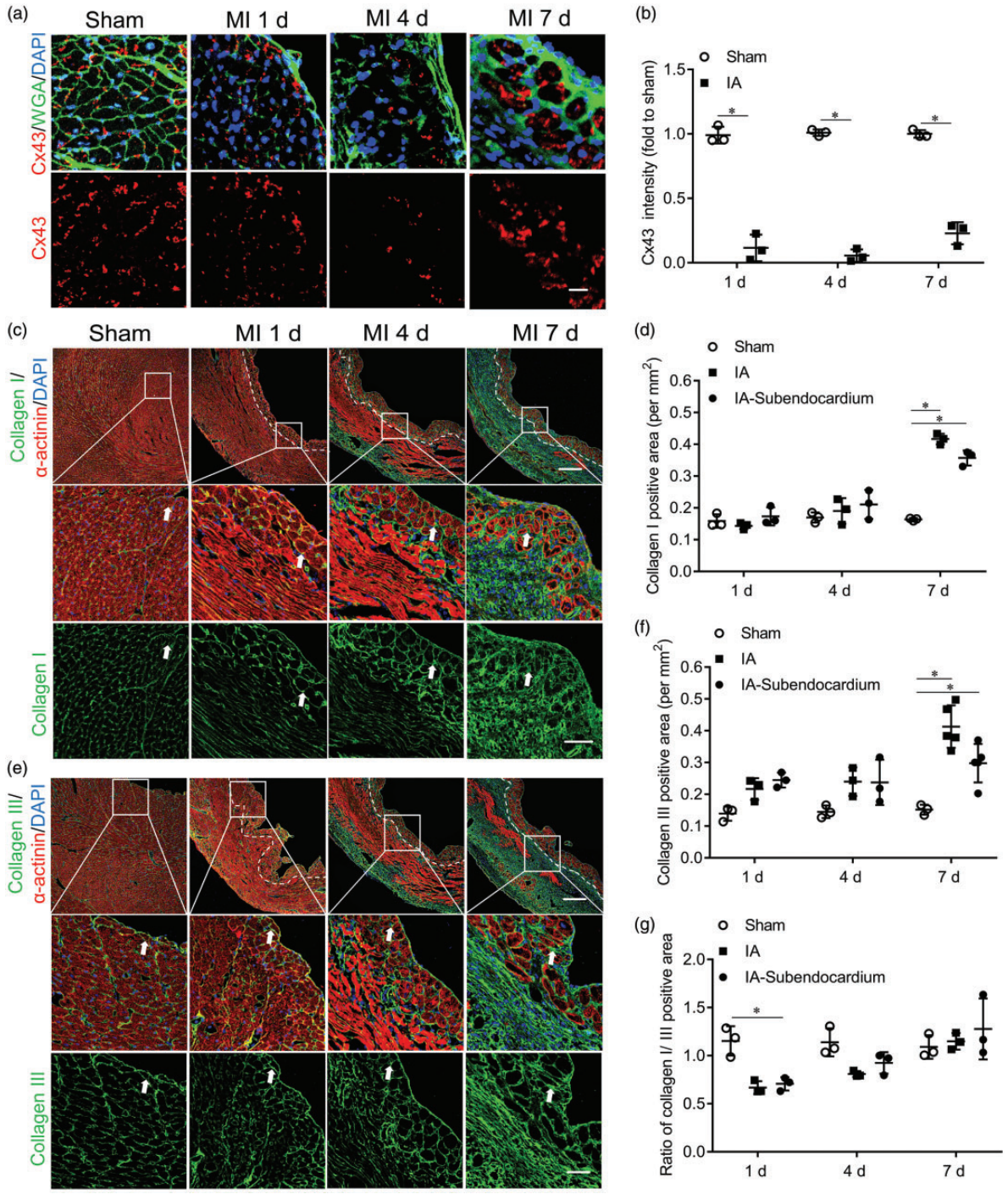

Figure 4. ECM remodeling in the subendocardial region of ischemic myocardium. (a) Co-immunofluorescent staining of Cx43 (red) and WGA (green). Nuclei are indicated by DAPI (blue). Scale bar, 20 μm. (b) Average optical density of Cx43 (fold to sham) in IA from day 1 to day 7 after LAD ligation. $^*P < 0.05$ between indicated groups. Co-immunofluorescent staining of type I (c) or III (e) collagen (green) with α-actinin (red). Nuclei are indicated by DAPI (blue). IA-subendocardial region is indicated by dotted line. White arrow indicates collagens which deposited around the surviving cardiomyocytes. Scale bar, 200 μm (up) and 50 μm (below). Quantification of collagen I (d) or III (f) positive area (per mm^2) in IA and IA-subendocardium from day 1 to day 7 after LAD ligation. $^*P < 0.05$ between indicated groups. (g) Ratio of collagen I/III positive area. $^*P < 0.05$ between indicated groups. (A color version of this figure is available in the online journal.)

heart.[11,12,27,28] Thus, the increase in collagen deposition would be ascribed to the activation of fibroblasts under the ischemic conditions.

The increase in LOX in the ECM of the subendocardial region was paralleled by the increased collagen deposition. On day 1, collagen III was increased causing a decrease in the ratio of collagen I/III, but LOX was decreased at this time suggesting the premature state of the ECM.[29] After that, the expression of LOX increased along with further increased deposition of both collagen I and III, and returning to the normal ratio of collagen I/III. LOX-catalyzed cross-linking of collagens is a repair process for the myocardium following ischemic injury.[8] After ischemia, surviving cardiomyocytes need to reconstitute their interaction

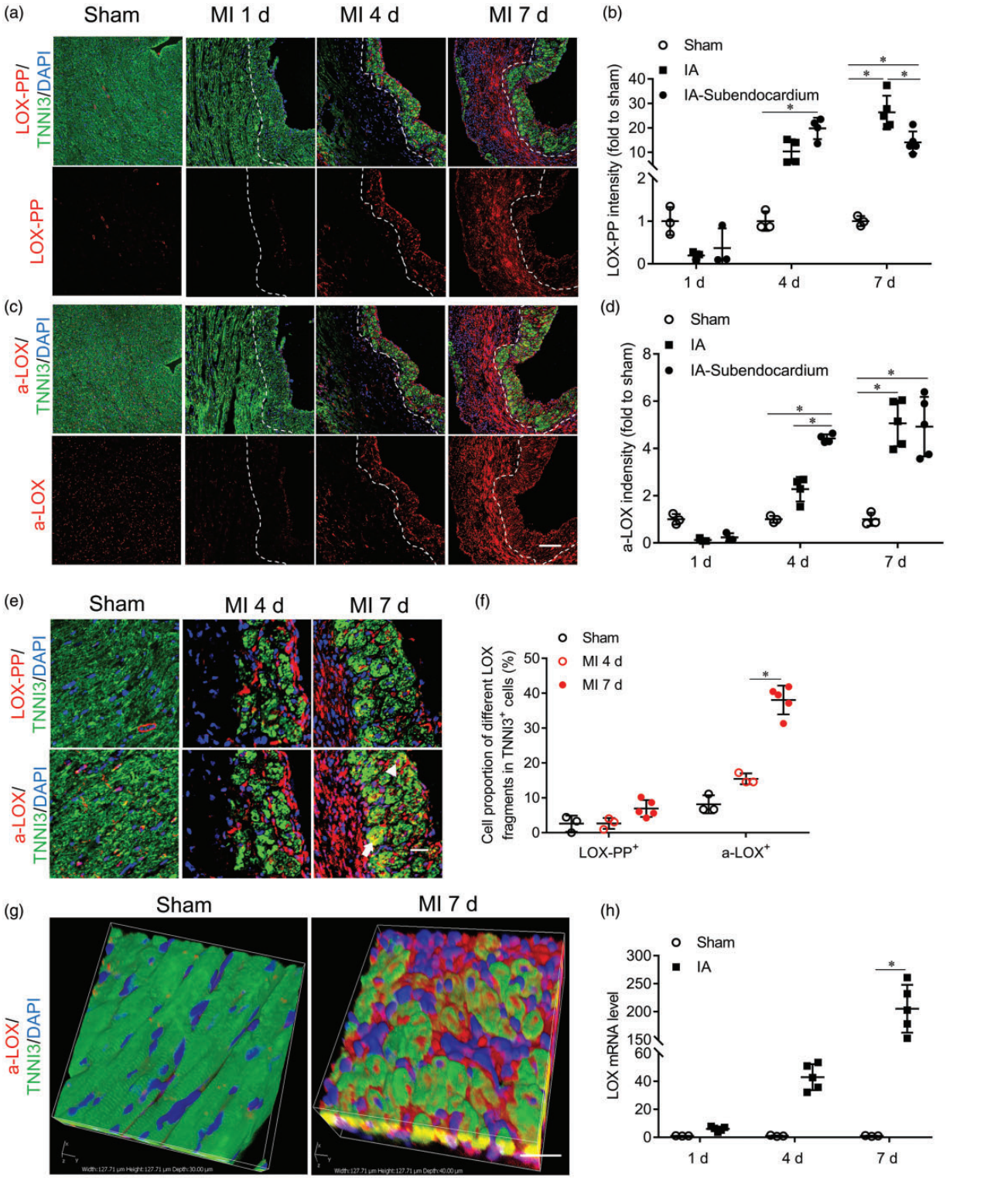

Figure 5. Changes of LOX in surviving cardiomyocytes in ischemic myocardium. Co-immunofluorescent staining of a-LOX (a) or LOX-PP (c) (red) with TNNI3 (green). Nuclei are indicated by DAPI (blue). IA-subendocardial region is indicated by dotted line. Scale bar, 100 μm. Average optical density of LOX-PP (b) or a-LOX (d) (fold to sham) in IA and IA-subendocardium from day 1 to day 7 after LAD ligation. *$P < 0.05$ between indicated groups. (e) Localization of LOX-PP (up, red) and a-LOX (below, red) in cardiomyocytes at day 4 and day 7 after LAD ligation. Cardiomyocytes are indicated by TNNI3 (green) and nuclei were indicated by DAPI (blue). White arrow indicates a-LOX within the cytosol of cardiomyocyte, and arrow head indicates a-LOX within the nucleus of cardiomyocyte. Scale bar, 20 μm. (f) Quantification of the cell proportion of cardiomyocytes within a-LOX (a-LOX$^+$) or LOX-PP (LOX-PP$^+$), *$P < 0.05$ between indicated groups. (g) 3D images of co-immunofluorescent staining of a-LOX (red) and TNNI3 (green). Nuclei are indicated by DAPI (blue). Scale bar, 20 μm. (h) Changes in LOX mRNA level from day 1 to day 7 after LAD ligation detected by qPCR. *$P < 0.05$ between indicated groups. (A color version of this figure is available in the online journal.)

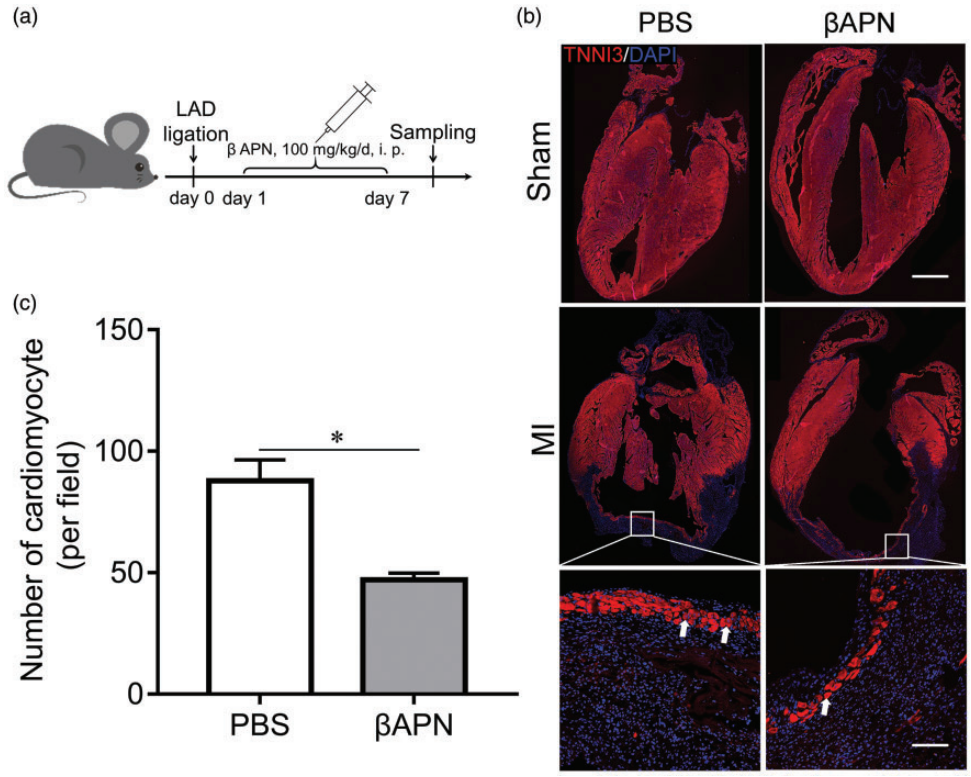

Figure 6. LOX inhibition reduced number of surviving cardiomyocytes. (a) Schematic diagram of the experiment protocol. (b) Immunofluorescent staining of cardiomyocytes (red). Cardiomyocytes are indicated by TNNI3 (red) and nuclei are indicated by DAPI (blue). Scale bar, 1000 μm and 100 μm. White arrow indicates the rounded cardiomyocyte. (c) Statistical analysis of surviving cardiomyocytes in the subendocardium, $^*P < 0.05$ between indicated groups. PBS: phosphate-buffered saline, as control. (A color version of this figure is available in the online journal.)

with the ECM, thus protecting them from anoikis.[30] In this context, the inhibition of LOX activity leading to an increased loss of cardiomyocytes suggests that the reestablishment or remodeling of the ECM by increased LOX would help cardiomyocyte survival. It seems that cross-linking of collagens is reversible, possibly related to the turnover of LOX and the activation of MMPs, as demonstrated in our previous studies.[12,27]

We observed that LOX-PP was only faintly detectable in the sham-operated myocardium, while it was dramatically increased after ischemia, suggesting its production was up-regulated after myocardial ischemia.[31,32] LOX is a kind of secretory protein, and is cleaved to become an activated LOX (a-LOX) and a LOX-PP peptide in the ECM.[31,33,34] The increase of a-LOX in the ECM along with the enhanced collagen deposition would be a disruptive alteration in cardiomyocyte communication and myocardial structural integrity.[14] We observed here that about 40% of the surviving cardiomyocytes contained a-LOX in their cytosol. It has been reported that a-LOX is not only relocated in the cytosol but also found in the nucleus.[35,36] Another report suggested that a-LOX can act as a transcription factor regulating target gene expression, such as collagen III in COS-7 cells.[37] The role of a-LOX as a transcription factor in cardiomyocytes has not been identified, but it might be that the increase in a-LOX is related to the up-regulation of collagen III, as observed in the present study.

In summary, the present study demonstrates that the excessive collagen deposition in the ECM along with the increase of a-LOX would substitute for the space emptied by the rounded-up or lost cardiomyocytes in the subendocardial region, and the altered ECM in turn helps survival of these cardiomyocytes in the hazardous environment. Thus, the ECM remodeling is correlated with the deformation of cardiomyocytes, and the electrical disconnection between the surviving cardiomyocytes due to Cx43 depletion and the increase in LOX would help these deformed cardiomyocytes to survive under ischemic conditions.

AUTHORS' CONTRIBUTIONS

All authors participated in the experimental design, interpretation of the results, and review of the manuscript; QC, YX, and XS were involved in the experimentation; QC and YX performed data analysis; YJK, QC, and YX wrote the manuscript, and YJK edited and approved the final version of the manuscript.

DECLARATION OF CONFLICTING INTERESTS

The author(s) declared no potential conflicts of interest with respect to the research, authorship, and/or publication of this article.

FUNDING

The author(s) disclosed receipt of the following financial support for the research, authorship, and/or publication of this article: We would like to appreciate the National Nature

Science Foundation of China (NSFC 81300109) for the financial support.

ORCID ID

Y James Kang https://orcid.org/0000-0001-8449-7904

SUPPLEMENTAL MATERIAL

Supplemental material for this article is available online.

REFERENCES

1. Sun X, Cai J, Fan X, Han P, Xie Y, Chen J, Xiao Y, Kang YJ. Decreases in electrocardiographic R-wave amplitude and QT interval predict myocardial ischemic infarction in rhesus monkeys with left anterior descending artery ligation. *PLoS One* 2013;**8**:e71876
2. Nofi C, Bogatyryov Y, Dedkov EI. Preservation of functional microvascular bed is vital for long-term survival of cardiac myocytes within large transmural post-myocardial infarction scar. *J Histochem Cytochem* 2018;**66**:99–120
3. Kobayashi K, Maeda K, Takefuji M, Kikuchi R, Morishita Y, Hirashima M, Murohara T. Dynamics of angiogenesis in ischemic areas of the infarcted heart. *Sci Rep* 2017;**7**:7156
4. Forman R, Cho S, Factor SM, Kirk ES. Acute myocardial infarct extension into a previously preserved subendocardial region at risk in dogs and patients. *Circulation* 1983;**67**:117–24
5. Lopez B, Querejeta R, Gonzalez A, Beaumont J, Larman M, Diez J. Impact of treatment on myocardial lysyl oxidase expression and collagen cross-linking in patients with heart failure. *Hypertension* 2009;**53**:236–42
6. Lin BL, Song T, Sadayappan S. Myofilaments: movers and rulers of the sarcomere. *Compr Physiol* 2017;**7**:675–92
7. Ali H, Braga L, Giacca M. Cardiac regeneration and remodelling of the cardiomyocyte cytoarchitecture. *FEBS J* 2020;**287**:417–38
8. Lopez B, Gonzalez A, Hermida N, Valencia F, de Teresa E, Diez J. Role of lysyl oxidase in myocardial fibrosis: from basic science to clinical aspects. *Am J Physiol Heart Circ Physiol* 2010;**299**:H1–9
9. Leybaert L, Lampe PD, Dhein S, Kwak BR, Ferdinandy P, Beyer EC, Laird DW, Naus CC, Green CR, Schulz R. Connexins in cardiovascular and neurovascular health and disease: pharmacological implications. *Pharmacol Rev* 2017;**69**:396–478
10. Manring HR, Dorn LE, Ex-Willey A, Accornero F, Ackermann MA. At the heart of inter- and intracellular signaling: the intercalated disc. *Biophys Rev* 2018;**10**:961–71
11. Xie Y, Chen J, Han P, Yang P, Hou J, Kang YJ. Immunohistochemical detection of differentially localized up-regulation of lysyl oxidase and down-regulation of matrix metalloproteinase-1 in rhesus monkey model of chronic myocardial infarction. *Exp Biol Med (Maywood)* 2012;**237**:853–9
12. Xiao Y, Nie X, Han P, Fu H, Kang YJ. Decreased copper concentrations but increased lysyl oxidase activity in ischemic hearts of rhesus monkeys. *Metallomics* 2016;**8**:973–80
13. Gonzalez-Santamaria J, Villalba M, Busnadiego O, Lopez-Olaneta MM, Sandoval P, Snabel J, Lopez-Cabrera M, Erler JT, Hanemaaijer R, Lara-Pezzi E, Rodriguez-Pascual F. Matrix cross-linking lysyl oxidases are induced in response to myocardial infarction and promote cardiac dysfunction. *Cardiovasc Res* 2016;**109**:67–78
14. Al-U'datt D, Allen BG, Nattel S. Role of the lysyl oxidase enzyme family in cardiac function and disease. *Cardiovasc Res* 2019;**115**:1820–37
15. Li K, Li C, Xiao Y, Wang T, Kang YJ. The loss of copper is associated with the increase in copper metabolism MURR domain 1 in ischemic hearts of mice. *Exp Biol Med (Maywood)* 2018;**243**:780–5
16. Hoffman JI. Transmural myocardial perfusion. *Prog Cardiovasc Dis* 1987;**29**:429–64
17. Algranati D, Kassab GS, Lanir Y. Why is the subendocardium more vulnerable to ischemia? A new paradigm. *Am J Physiol Heart Circ Physiol* 2011;**300**:H1090–100
18. Smyth JW, Shaw RM. Autoregulation of connexin43 gap junction formation by internally translated isoforms. *Cell Rep* 2013;**5**:611–8
19. Macquart C, Juttner R, Morales Rodriguez B, Le Dour C, Lefebvre F, Chatzifrangkeskou M, Schmitt A, Gotthardt M, Bonne G, Muchir A. Microtubule cytoskeleton regulates connexin 43 localization and cardiac conduction in cardiomyopathy caused by mutation in A-type lamins gene. *Hum Mol Genet* 2019;**28**:4043–52
20. Dai W, Nadadur RD, Brennan JA, Smith HL, Shen KM, Gadek M, Laforest B, Wang M, Gemel J, Li Y, Zhang J, Ziman BD, Yan J,AX, Beyer EC, Lakata EG, Kasthuri N, Efimov IR, Broman MT, Moskowitz IP, Shen L, Weber CR. ZO-1 regulates intercalated disc composition and atrioventricular node conduction. *Circ Res* 2020;**127**:e28–43
21. Basheer WA, Xiao S, Epifantseva I, Fu Y, Kleber AG, Hong T, Shaw RM. GJA1-20k arranges actin to guide Cx43 delivery to cardiac intercalated discs. *Circ Res* 2017;**121**:1069–80
22. Liu L, Yan M, Yang R, Qin X, Chen L, Li L, Si J, Li X, Ma K. Adiponectin attenuates lipopolysaccharide-induced apoptosis by regulating the Cx43/PI3K/AKT pathway. *Front Pharmacol* 2021;**12**:644225
23. Gajarsa JJ, Kloner RA. Left ventricular remodeling in the post-infarction heart: a review of cellular, molecular mechanisms, and therapeutic modalities. *Heart Fail Rev* 2011;**16**:13–21
24. Yuan X, Scott IC, Wilson MD. Heart enhancers: Development and disease control at a distance. *Front Genet* 2021;**12**:642975
25. Wang WE, Li L, Xia X, Fu W, Liao Q, Lan C, Yang D, Chen H, Yue R, Zeng C, Zhou L, Zhou B, Duan DD, Chen X, Houser SR, Zeng C. Dedifferentiation, proliferation, and redifferentiation of adult mammalian cardiomyocytes after ischemic injury. *Circulation* 2017;**136**:834–48
26. Beardslee MA, Laing JG, Beyer EC, Saffitz JE. Rapid turnover of connexin43 in the adult rat heart. *Circ Res* 1998;**83**:629–35
27. Liu Y, Xiao Y, Liu J, Feng L, Kang YJ. Copper-induced reduction in myocardial fibrosis is associated with increased matrix metalloproteins in a rat model of cardiac hypertrophy. *Metallomics* 2018;**10**:201–8
28. Xiao Y, Liu Y, Liu J, Kang YJ. The association between myocardial fibrosis and depressed capillary density in rat model of left ventricular hypertrophy. *Cardiovasc Toxicol* 2018;**18**:304–11
29. Canelon SP, Wallace JM. Substrate strain mitigates effects of beta-aminopropionitrile-induced reduction in enzymatic crosslinking. *Calcif Tissue Int* 2019;**105**:660–9
30. Imanaka-Yoshida K. Tenascin-C in cardiovascular tissue remodeling: from development to inflammation and repair. *Circ J* 2012;**76**:2513–20
31. Kagan HM, Li W. Lysyl oxidase: properties, specificity, and biological roles inside and outside of the cell. *J Cell Biochem* 2003;**88**:660–72
32. Rosini S, Pugh N, Bonna AM, Hulmes DJS, Farndale RW, Adams JC. Thrombospondin-1 promotes matrix homeostasis by interacting with collagen and lysyl oxidase precursors and collagen cross-linking sites. *Sci Signal* 2018;**11**:eaar2566
33. Noda K, Kitagawa K, Miki T, Horiguchi M, Akama TO, Taniguchi T, Taniguchi H, Takahashi K, Ogra Y, Mecham RP, Terajima M, Yamauchi M, Nakamura T. A matricellular protein fibulin-4 is essential for the activation of lysyl oxidase. *Sci Adv* 2020;**6**:eabc1404
34. Calabro NE, Barrett A, Chamorro-Jorganes A, Tam S, Kristofik NJ, Xing H, Loye AM, Sessa WC, Hansen K, Kyriakides TR. Thrombospondin-2 regulates extracellular matrix production, LOX levels, and cross-linking via downregulation of miR-29. *Matrix Biol* 2019;**82**:71–85
35. Liu N, Cox TR, Cui W, Adell G, Holmlund B, Ping J, Jarlsfelt I, Erler JT, Sun XF. Nuclear expression of lysyl oxidase enzyme is an independent prognostic factor in rectal cancer patients. *Oncotarget* 2017;**8**:60015–24
36. Li W, Nellaiappan K, Strassmaier T, Graham L, Thomas KM, Kagan HM. Localization and activity of lysyl oxidase within nuclei of fibrogenic cells. *Proc Natl Acad Sci U S A* 1997;**94**:12817–22
37. Giampuzzi M, Botti G, Di Duca M, Arata L, Ghiggeri G, Gusmano R, Ravazzolo R, Di Donato A. Lysyl oxidase activates the transcription activity of human collagene III promoter. Possible involvement of Ku antigen. *J Biol Chem* 2000;**275**:36341–9

(Received March 10, 2021, Accepted August 6, 2021)